Notes

Crystal Orientation within Lamellae-Forming Block Copolymers of Semicrystalline Poly(4-vinylpyridine)-*b*-poly(ϵ-caprolactone)

Ya-Sen Sun,[†] Tsai-Ming Chung,[‡] Yi-Jing Li,[‡] Rong-Ming Ho,*[,‡] Bao-Tsan Ko,[§] and U-Ser Jeng[†]

National Synchrotron Radiation Research Center, Hsinchu 30076, Taiwan; Department of Chemical Engineering, National Tsing-Hua University, Hsinchu 30013, Taiwan; and Material and Chemical Research Laboratories, Industrial Technology Research Institute, Hsinchu 30013, Taiwan

Received April 27, 2007
Revised Manuscript Received June 27, 2007

Introduction

Because of diverse morphologies upon controls over compositions and segregation strength limits of constituting blocks, semicrystalline diblock copolymers have been employed as templates to explore the crystallization behavior of polymer chains confined in nanoscale space provided that crystallizable blocks crystallize within preexisting microdomains (MD) driven by microphase separation, for which the crystallization temperature T_C lies below the temperature T_{ODT} for the order−disorder transition.[1−16] The number of available possible conformations reduces because the restricted geometries imposed on crystallizing polymer materials are on a nanometer scale, which is approximately the length of a polymer chain in coil form.[3−16] Therefore, the nanoscaled confinement size plays an important role in crystallization kinetics.[9e,16,17] Our previous work indicated that a distinct transformation of isothermal crystallization kinetics, from heterogeneous to homogeneous nucleation, occurred between two neighboring glassy lamellar layers when the confined size became less than 8 nm (equivalent to the size of forming a stable nucleus via heterogeneous nucleation), leading to an abrupt shift in crystallization to a low-temperature region.[16] On the other hand, altering the confined size led to variances in crystallographic orientation upon changing confined space.[9e,16] In this extended Note, three distinct confined spaces of 6, 8.8, and 11 nm were constructed upon varying the molar mass of diblock copolymers to explore a correlation between crystal orientations and confined spaces within vitrified lamellar MD of crystalline−amorphous (C−A) block copolymers in strong segregation limits with T_{ODT} (order−disorder transition temperature of the microphase separation) $\gg T_g^a$ (glass transition temperature of the amorphous block) > T_C^c (crystallization temperature of crystallizable blocks). In addition to the perpendicular and random orientations for the 11 and 6 nm confined sizes reported previously,[16] the parallel orientation found at an intermediate level of confinement (8.8 nm) was analyzed in detail.

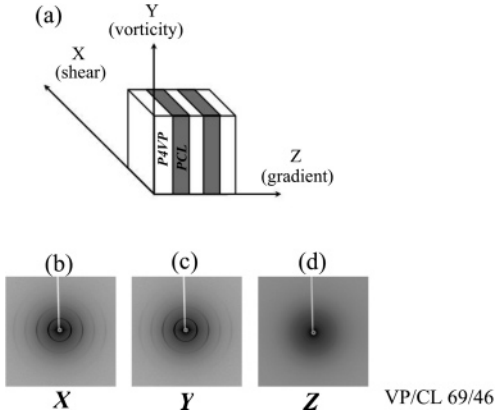

Figure 1. (a) Geometry of the rimming-flow induced P4VP−PCL copolymers with a lamellar MD. Sets of 2D SAXS patterns of VP/CL 69/46 at 80 °C with the X-ray beam along directions (b) *X*, (c) *Y*, and (d) *Z*.

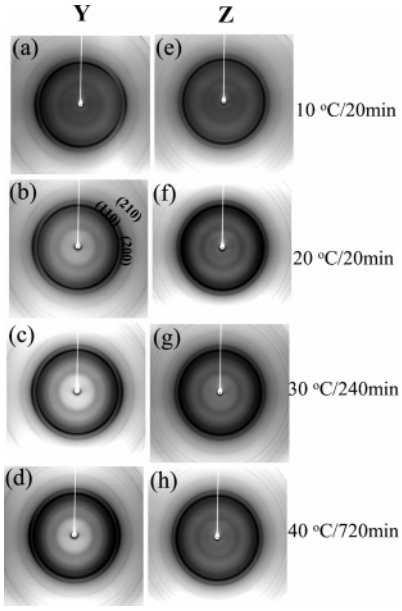

Figure 2. 2D WAXD patterns of oriented VP/CL 69/46 samples isothermally crystallized at 10 (a, e), 20 (b, f), 30 (c, g), and 40 °C (d, h). The left WAXD patterns were recorded with the beam along the *Y*-direction and the right ones along the *Z*-direction.

Experiments

Materials. Three P4VP−PCL block copolymers of VP/CL 146/91, 69/46, and 56/38 were used to explore the crystal orientation and melting behavior under nanoscale confinement; the PCL domains had thicknesses 11 (VP/CL 146/91), 8.8 (VP/CL 69/46), and 6 nm (VP/CL 56/38). The detailed synthetic routes and characterizations of the synthesized copolymers were described elsewhere.[16] All bulk samples of block copolymers with long-range

* To whom correspondence should be addressed: e-mail rmho@mx.nthu.edu.tw; Tel 886-3-5738349; Fax 886-3-5715408.
[†] National Synchrotron Radiation Research Center.
[‡] National Tsing-Hua University.
[§] Industrial Technology Research Institute.

10.1021/ma0709708 CCC: $37.00
Published on Web 08/10/2007

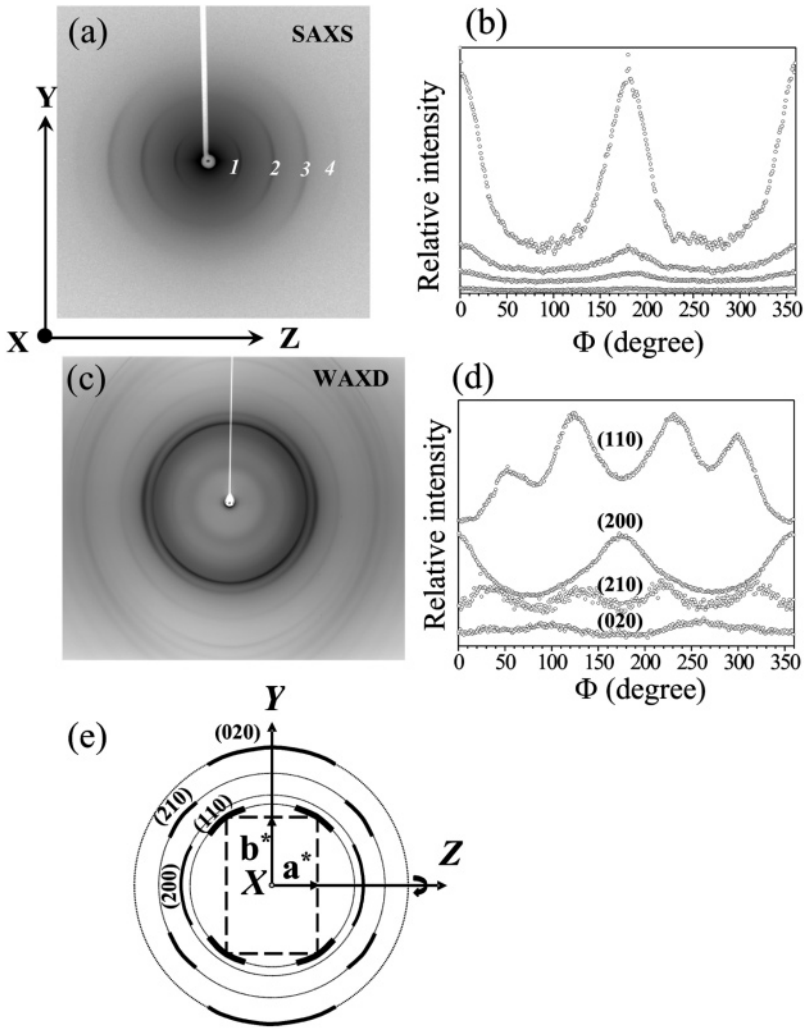

Figure 3. X-ray patterns of oriented VP/CL 69/46 samples isothermally crystallized at 20 °C from an ordered melt at 80 °C: (a) a 2D SAXS pattern with the beam parallel to the *X* direction, (b) corresponding azimuthal profiles for the 2D SAXS pattern, (c) a 2D WAXD pattern along the *X* direction, (d) corresponding azimuthal profiles for the 2D WAXD pattern, and (e) corresponding reflections are indicated as shown in schematic of the 2D WAXD pattern.

aligned microphase-separated lamellar MD were prepared by a rimming coating process, followed by thermal annealing at 140 °C for 12 h to eliminate possible effects of PCL crystallization and residual solvent on MD during the rimming coating process.

Equipment and Experiments. Before we applied SAXS to characterize the microphase-separated lamellar morphology of P4VP−PCL copolymers, we subjected the samples to thermal treatments in a DSC. 2D SAXS experiments were performed at the BL01B SWLS beamline (λ = 1.180 95 Å) at the National Synchrotron Radiation Research Center (NSRRC), Taiwan. 2D SAXS images were collected on Fuji plates. The scattering vector was calibrated by linear regression over the positions of numerous orders of the long spacing of silver behenate, with $q = 1.076\ \text{nm}^{-1}$; $q = (4\pi/\lambda)\sin(\theta/2)$, with scattering angle θ. The sample cells were sealed with two pieces of Kapton. The 2D SAXS patterns were accumulated for 2 min each. SAXS experiments for isothermal melt crystallization were performed *in situ* in a hot stage under a nitrogen atmosphere. Static WAXD experiments were performed at the wiggler 17A1 beamline (λ = 1.332 95 Å). 2D WAXD images were collected for 2 min for each data acquisition and were calibrated using α-Al_2O_3. A contribution from air scattering was subtracted from both 2D SAXS and WAXD patterns.

Results and Discussion

Oriented samples were examined by SAXS with X-ray beam along the shear, vorticity, and gradient directions, designated *X*, *Y*, and *Z*, respectively. The orientation of the microphase-separated lamellar MD was identified by the strongly anisotropic patterns along both *X* and *Y* directions, whereas only isotropic powder rings with weak intensities were observed along the *Z* direction (as illustrated in Figure 1 for VP/CL 69/46). The *X* and *Y* directions are notably identical. Similar results can be found in all amorphous P4VP−PCL diblock copolymers studied at which the reflections can be identified at multiple integrals of the first principal peak, indicative of lamellar phase morphology with long-range orientation and order.

For the oriented samples, VP/CL 146/91, crystallized at various T_C in a range 20−45 °C (as shown in Figure S1 of Supporting Information), the 2D WAXD patterns reveal strongly anisotropic patterns (like a fiber pattern) along the *Y* direction but isotropic patterns (like a powder ringed pattern) along the *Z* direction. Since all PCL orthorhombic crystals within the 11 nm lamellar MD adopt the perpendicular-type orientation with respect to the lamellar plane regardless of T_C in the typical region of crystallization temperature, 20−45 °C, the crystallographic fiber pattern of perpendicularly oriented PCL crystals reveals all the (*hk*0) reflections appearing along the meridian direction (i.e., shear direction). Therefore, the observed reflections are indexed as (110), (200), and (210) on the basis of an orthorhombic crystal structure of PCL with a = 0.7096 nm, b = 0.4974 nm, c = 1.7297 nm, and $\alpha = \beta = \gamma = 90°$.[18] This implies that the chain (*c*-axis) of PCL crystalline lamellae is

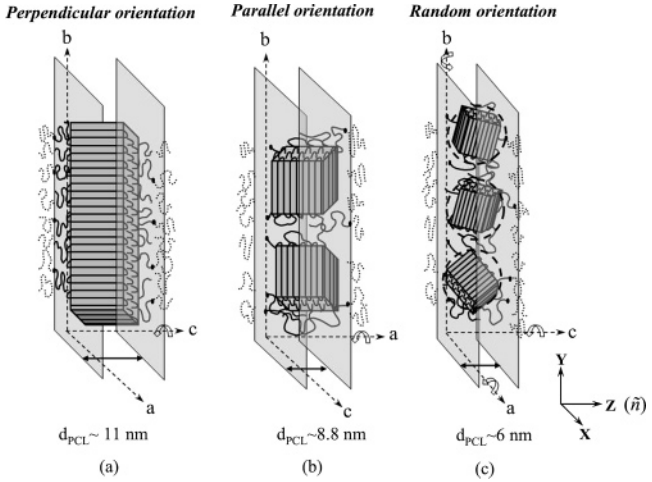

Figure 4. Three schematic presentations of chains orientation under confinement with various spaces in the corresponding diblock copolymers: (a) VP/CL 146/91, (b) VP/CL 69/46, and (c) VP/VL 56/38. Individual confined spaces are listed in the figure.

oriented parallel to the microphase-separated lamellar normal ($\tilde{n}$) whereas *a*- and *b*-axes are in the $X-Y$ plane.

It is intriguing to analyze the crystal orientation generated when the confining size becomes 8.8 nm, which value is identical to the correlation length of crystalline PCL lamellae with a perpendicular orientation.[19] The WAXD patterns for VP/CL 69/46 crystallized at 10, 20, 30, and 40 °C are shown in Figure 2; Figures 2a−d were recorded along the *Y* direction and Figures 2e−h along the *Z* direction. As shown in Figure 2, the 2D WAXD patterns reveal a strong anisotropy along the *Y* direction but isotropy (powder ring patterns) along the *Z* direction. The azimuthal profiles of these reflections in the 2D SAXS and corresponding WAXD patterns, with both taken along the *X* direction (Figures 3a,c) are accordingly shown in Figures 3b,d. For the pattern shown in Figure 3b, the maximum intensities of all observed scatterings occur at the azimuthal angle, $\Phi = 0°$ and 180°. The WAXD pattern in Figure 3d shows that the maximum diffraction intensity of the (110) reflection is located at the azimuthal angles, $\Phi = 53°$, 125°, 231°, and 300°, that of the (200) reflection is at $\Phi = 0°$ and 180°, that of the (210) reflections is at $\Phi = 34°$, 125°, 217°, and 321°, and that of the (020) reflection is at $\Phi = 90°$ and 270°. As shown in the schematic of the 2D WAXD pattern (Figure 3e), the pattern displays two meridional (020) reflections, two equatorial (200) reflections, and two sets of quadrantal (110) and (210) reflections. According to the SAXS and WAXS patterns, we propose that, for the crystallized VP/CL 69/46, the *c*-axis of the PCL crystals is oriented parallel to the lamellar surface in the temperature range 10−40 °C.

The crystallographic orientation of crystallites grown under confinement is affected by several factors, such as confined size and shape[9e,f] and interplay among the segregation strength,[10−12,14] the crystallization temperature,[9d] and the glass-transition temperature of the confining block.[9a,b] A large confined space, such as 11 nm, allows the PCL crystallites to achieve a perpendicular orientation (Figure 4a). A decreased confined space strongly frustrates crystallization with folded chains normal to the layers: for a 8.8 nm confined space, the orientation must alter from perpendicular to parallel to accommodate the space at most accessible temperatures (Figure 4b), 10−40 °C; otherwise, the crystalline lamellar thickness must be greatly diminished, in which case significantly depressed endothermic peaks are expected to be observed in DSC.[15c] For example, if the crystalline lamellar stems adopted a perpendicular orientation within a confining space of 8.8 nm, the thickness should be ca. 2.82 nm according to a crystallinity 0.32. Such thin crystalline lamellae would melt at low temperatures upon heating in a DSC. The endotherms observed in DSC for VP/CL 69/46 are only slightly less than the corresponding homopolymer hCL 46 having a similar molar mass.

Because of the extremely small confined size of 6 nm, the PCL blocks for VP/CL 56/38 remain amorphous in the typical crystallization temperature region 10−45 °C; for this reason polymer crystallization is effected only in a low-temperature range −10 to −30 °C. For a confined space decreasing to 6 nm, all 2D WAXD patterns taken along *Y* and *Z* directions are isotropic (ring reflection): the crystal orientation within the confined lamellae is random (see Figure S2 of Supporting Information) (Figure 4c). Homogeneous nucleation hence dominates the overall crystallization kinetics in this temperature range, confirmed by TEM of VP/CL 56/38 melt-crystallized at −10 °C in our previous work.[16] As a result, with a varied confined space PCL crystals develop in three orientations (see Figure 4 for illustration).

Conclusion

For the 11 nm confinement space with hard confinement and strong segregation, each PCL domain was found to accommodate perpendicularly oriented PCL crystallites. An altered confinement from 11 to 8.8 nm produces a transformation in crystallographic orientation, from perpendicular to parallel type. This change reflects that the decrease in confined space retards the rate of crystal growth more significantly when the chain axis is parallel to the lamellar normal than when it is parallel to the lamellar surface. The parallel-type orientation is allowable for one-dimensional crystal growth. Once the confined space is lower than 6 nm, the crystal orientation will be lost at deep undercoolings. Therefore, perpendicular, parallel, and random orientation can be achieved in response to progressively decreasing confined size.

Acknowledgment. We thank the National Science Council for support (NSC-95-2221-E-007-131-MY2) and also acknowledge Dr. Ying-Hung Lai for his assistance in the SAXS experiments at beamline BL01B at the NSRRC.

Supporting Information Available: WAXD data for the VP/CL 146/91 and 56/38 samples crystallized at various temperatures. This material is available free of charge via the Internet at http://pubs.acs.org.

References and Notes

(1) Bates, F. S.; Fredrickson, G. H. *Annu. Rev. Phys. Chem.* **1990**, *41*, *525*.

(2) Hamley, I. W. *The Physics of Block Copolymers*; Oxford University Press: New York, 1998; Chapter 5.

(3) (a) Whitmore, M. D.; Noolandi, J. *Macromolecules* **1988**, *21*, 1482. (b) DiMarzio, E. A.; Guttman, C. M.; Hoffman, J. D. *Macromolecules* **1980**, *13*, 1194.

(4) Nojima, Kato, S.; Yamamoto, K. S.; Ashida, T. *Macromolecules* **1992**, *25*, 2237.

(5) (a) Rangarajan, P.; Register, R. A.; Fetters, L. J.; Bras, W.; Naylor, S.; Ryan, A. J. *Macromolecules* **1995**, *28*, 4932. (b) Rangarajan, P.; Register, R. A.; Fetters, L. J. *Macromolecules* **1993**, *26*, 4640. (c) Loo, Y. L.; Register, R. A.; Adamson, D. H. *Macromolecules* **2000**, *33*, 8361. (d) Loo, Y. L.; Register, R. A.; Ryan, A. J. *Macromolecules* **2002**, *35*, 2365. (e) Loo, Y. L.; Register, R. A.; Ryan, A. J. *Phys. Rev. Lett.* **2000**, *84*, 4120. (f) Loo, Y. L.; Register, R. A.; Ryan, A. J.; Dee, G. T. *Macromolecules* **2001**, *34*, 8968.

(6) (a) Chen, H. L.; Hsiao, S. C.; Lin, T. L.; Yamauchi, K.; Hasegawa, H.; Hashimoto, T. *Macromolecules* **2001**, *34*, 671. (b) Chen, H. L.; Wu, J. C.; Lin, T. L.; Lin, J. S. *Macromolecules* **2001**, *34*, 6936.

(7) Reiter, G.; Castelein, G.; Sommer, J. U.; Rollele, A.; Thurn-Albrecht, T. *Phys. Rev. Lett.* **2001**, *87*, 226101.
(8) Rangarajan, P.; Register, R. A.; Adamson, D. H.; Fetters, L. J.; Bras, W.; Naylor, S.; Ryan, A. J. *Macromolecules* **1995**, *28*, 1422.
(9) (a) Zhu, L.; Chen, Y.; Zhang, A.; Calhoun, B. H.; Chum, M.; Quirk, R. P.; Cheng, S. Z. D.; Hsiao, B. S.; Yeh, F.; Hashimoto, T. *Phys. Rev. B* **1999**, *60*, 10022. (b) Zhu, L.; Cheng, S. Z. D.; Calhoun, B. H.; Ge, Q.; Quirk, R. P.; Thomas, E. L.; Hsiao, B. S.; Yeh, F.; Lotz, B. *Polymer* **2001**, *42*, 5829. (c) Zhu, L.; Cheng, S. Z. D.; Calhoun, B. H.; Ge, Q.; Quirk, R. P.; Thomas, E. L.; Lotz, B.; Hsiao, B. S.; Yeh, F.; Liu, L. *Macromolecules* **2001**, *34*, 1244. (d) Zhu, L.; Cheng, S. Z. D.; Calhoun, B. H.; Ge, Q.; Quirk, R. P.; Thomas, E. L.; Hsiao, B. S.; Yeh, F.; Lotz, B. *J. Am. Chem. Soc.* **2000**, *122*, 5957. (e) Huang, P.; Zhu, L.; Gau, Y.; Ge, Q.; Jing, A. J.; Chen, W. Y.; Quirk, R. P.; Cheng, S. Z. D.; Thomas, E. L.; Lotz, B.; Hsiao, B. S.; Avila-Orta, C. A.; Sics, I. *Macromolecules* **2004**, *37*, 3689. (f) Huang, P.; Gau, Y.; Quirk, R. P.; Ruan, J.; Lotz, B.; Thomas, E. L.; Hsiao, B. S.; Avila-Orta, C. A.; Sics, I.; Cheng, S. Z. D. *Polymer* **2006**, *47*, 5457.
(10) (a) Ryan, A. J.; Hamley, I. W.; Bras, W.; Bates, F. S. *Macromolecules* **1995**, *28*, 3860. (b) Hamley, I. W.; Fairclough, J. P. A.; Terrill, N. J.; Ryan, A. J.; Lipic, P. M.; Bates, F. S.; Towns-Andrews, E. *Macromolecules* **1996**, *29*, 8835.
(11) Lotz, B.; Kovacs, A. J. *Kolloid Z. Z. Polym.* **1966**, *209*, 97.
(12) (a) Cohen, R. E.; Bellare, A.; Drzewinski, M. A. *Macromolecules* **1994**, *27*, 2321. (b) Douzinas, K. C.; Cohen, R. E.; Halasa, A. F. *Macromolecules* **1991**, *24*, 4457. (c) Douzinas, K. C.; Cohen, R. E. *Macromolecules* **1992**, *25*, 5030.
(13) (a) Müller, A. J.; Albuerne, J.; Marquez, L.; Raquez, J. M.; Degée, P.; Dubois, P.; Hobbs, J.; Hamley, I. W. *Faraday Discuss.* **2005**, *128*, 231. (b) Müller, A. J.; Albuerne, J.; Esteves, L. M.; Marquez, L.; Raquez, J. M.; Degée, P.; Dubois, P.; Collins, S.; Hamley, I. W. *Macromol. Symp.* **2004**, *215*, 369. (c) Müller, A. J.; Balsamo, V. M.; Arnal, L.; Jakob, T.; Schmalz, H.; Abetz, V. *Macromolecules* **2002**, *35*, 3048.
(14) Koo, C. M.; Wu, L.; Lim, L. S.; Mahanthappa, M. K.; Hillmyer, M. A.; Bates, F. S. *Macromolecules* **2005**, *38*, 6090.
(15) (a) Ho, R. M.; Lin, F. H.; Tsai, C. C.; Lin, C. C.; Ko, B. T.; Hsiao, B. S.; Sics, I. *Macromolecules* **2004**, *37*, 5985. (b) Ho, R. M.; Chiang, Y. W.; Lin, C. C.; Huang, B. H. *Macromolecules* **2005**, *38*, 4769. (c) Chung, T. M.; Ho, R. M.; Kuo, J. C.; Tsai, J. C.; Hsiao, B. S.; Sics, I. *Macromolecules* **2006**, *39*, 2739. (d) Ho, R.-M.; Chung, T.-M.; Tsai, J.-C.; Kuo, J.-C.; Hsiao, B. S.; Sics, I. *Macromol. Rapid Commun.* **2005**, *26*, 107.
(16) Sun, Y. S.; Chung, T. M.; Li, Y. J.; Ho, R. M.; Ko, B. T.; Jeng, U. S.; Lotz, B. *Macromolecules* **2006**, *39*, 5782.
(17) Woo, E.; Huh, J.; Jeong, Y. G.; Shin, K. *Phys. Rev. Lett.* **2007**, *98*, 136103.
(18) (a) Hu, H.; Dorset, D. L. *Macromolecules* **1990**, *23*, 4604. (b) Bittiger, H.; Marchessault, R. H.; Niegisch, W. D. *Acta Crystallogr.* **1970**, *B26*, 1923.
(19) Unlike PCL homopolymers having diverse lamellar stacks with long periods in a range 11−13 nm, VP/CL 146/91 has a lamellae-within-lamellae structure, in which periodic PCL crystallites with small periods, with thicknesses ca. 8.6−8.8 nm, are obtained through spatial confinement of 11 nm.

MA0709708